Aerodynamic Performance Characterization of Slotted Propeller: Part B Effect of Angle

Aravind SEENI*

*Corresponding author
School of Aerospace Engineering, University of Science Malaysia,
Engineering Campus, Nibong Tebal, Penang 14300, Malaysia,
aravindseeni@gmail.com

DOI: 10.13111/2066-8201.2019.11.4.14

Received:11 September 2019/ Accepted: 01 October 2019/ Published: December 2019
Copyright © 2019. Published by INCAS. This is an "open access" article under the CC BY-NC-ND license (http://creativecommons.org/licenses/by-nc-nd/4.0/)

Abstract: *In this paper, designs of slotted propeller blade were discussed numerically, in terms of aerodynamic performance and static structural analysis. Baseline APC Slow Flyer 10' x 7' small scale propeller blade was modified by including slots along the propeller blade. Numerical analysis has been done to determine the influence of slots angle towards thrust coefficient, power coefficient and efficiency. Simulations were performed by using ANSYS Fluent implementing k-ω turbulence model and Multiple Reference Frame to incorporate rotational speed of the propeller. The analyses were conducted at a fixed rotational speed, with variance of advance ratio. Initial slotted design is set at 180 degree and the angles were changed with 10-degree interval, ranging from 180 degree to 90 degree. The results were compared with available experimental data. For the slotted design, the result shows that inducing slots do not always lead to improvement in propeller blade performance. Improvement in thrust coefficient with the range of 0.267% to 2.71% can be seen for low advance ratio for most of slot angles. However, a significant increase in power coefficient can be observed which reduces the overall efficiency of the propeller blade. For stress and deformation, ANSYS Mechanical Static Structure was used to determine maximum Von-Mises stress, maximum Von-Mises strain, and total deformation. The analyses were conducted by using 60% long strand fiber glass reinforced nylon 6 Natural. The blade is more suitable to operate at higher velocity. At lower operational velocity, the blade tends to experience material failure as the stress exceeds stress at break.*

Key Words: *slotted propeller, computational fluid dynamics, static structural, low Reynolds number, APC Slow Flyer, ANSYS Fluent, ANSYS Mechanical*

1. INTRODUCTION

Unmanned Aerial Vehicle (UAV) development is influenced by technology growth over time. Upgrades of UAV systems and components have determined their use in a wide range of areas such as crop monitoring, herd monitoring, and crop dusting. Furthermore, many industries are utilizing UAV for monitoring and survey especially for mineral exploration, geophysical survey, oil and gas exploration [1] - [4].

Therefore, it is very important to design highly efficient UAV. Efficiency of a UAV is influenced by the propeller. Thus, propeller selected need to be able to cater the aerodynamic requirements of the UAV. Current UAV propeller optimization focuses on the conventional parameter, such as diameter, pitch, airfoil and blade angle. The implementation of

unconventional propeller design such as slotted, serration and tubercle blade are barely adopted for UAV. This is due to lack of available research and information for the design mentioned.

Hence, this study intends to design and study the performance of small scale slotted propeller blade design for low Reynolds number application. The propeller used for UAV has low Reynolds number, typically less than 100,000 measured at 75% chord at sea level conditions. This is due to its smaller size, and operating at low freestream advance speed but high Reynolds number.

The study is divided into two main analysis, including aerodynamic analysis and static structural analysis. The flow simulation is carried out by using commercial computational fluid dynamic (CFD) solver, FLUENT. Three dimensional CFD software employing Reynolds-averaged Navier Stokes (RANS) equations coupled with turbulence model to determine the thrust coefficient, power coefficient and efficiency was used. Meanwhile ANSYS Mechanical Structural was employed to determine the highest stress and maximum deformation along the propeller blade. Section below describes the propeller blade design available for aircraft, UAV, marine ship and wind turbine as the principle concept is the same varying on the design to suits the working fluid [5], [6].

Some of the unconventional designs are slotted, serrated and tubercle designs. The impact of leading edge and trailing edge serration has been tested by Liu et. al [7]. The results show that for both design tested, the lift coefficient reduces significantly, ranging from 15% to 40% from the baseline deign. Thus, it is concluded that implementation of serration into airfoil design will influence the overall aerodynamic performance. Chong et. al [8] performed an experiment to determine the effect of trailing edge serration for airfoil. The result shows that saw-tooth surface may trigger boundary layer separation near trailing edge of the airfoil, which will significantly influence the aerodynamic performance. In addition, Chong et al. [9] further investigate the influence of serration by incorporating several serration forms, including M-shaped, wavy, and sawtooth. Based on the analysis, it is proven that serration modifies boundary layer but at the same time improving in terms of aeroacoustics.

Ibrahim et al. [10] performed the analysis to determine the influence of slotted and tubercle design into the performance of wind turbine. The result shows that slotted design shows an improvement in terms of power compared to straight blade design only at lower speed. Meanwhile tubercle design shows conditional performance, with improvements at higher wind velocities. Lin et al. [11] study the performance of wave-like trailing edge wind turbine. The result shows improvement of 2.31% for maximum thrust, with 16.4% increase in power compared to straight blade design. Belamadi et al. [12] explore slotted airfoil for wind turbine blades. The designs were tested for different slot location, width and slope to determine optimize slotted airfoil. The result shows improvements only over specific range of angle of attack. In addition, the overall efficiency of the design is lower than baseline configuration due to increase in drag. Thus, it is concluded that implementation of slotted design does not always lead to performance improvements, as it depends on the position and size of the slots.

There are two methods available to determine the performance of propeller blade, including experimental and numerical. Both methods have been widely employed by many researches based on the suitability of the analysis. For propeller blade analysis, experimental method utilizes wind tunnel to collect propeller performance as discussed by Brandt et al. [13] and Deters et. al [14].

For numerical analysis, lots of research was performed by utilizing commercially available computational fluid dynamic software such as ANSYS Fluent and CFX. Subhas et al. [15] measure the performance by utilizing Fluent. The investigation is based on k-ε

turbulence model and multiple reference frame to incorporate rotational speed. The result shows reliable values with maximum and minimum difference of 0.0013 and 0.001 respectively. Wang et al. [16] performed similar method by incorporating boundary-layer transition model into the analysis. Improved results were obtained as compared to standard k-ω turbulence model. In addition, Benini[17] performed CFD analysis to determine the performance of propeller blade numerically. The method suggested in the study manages to display minimum error, with discrepancy of 5% in the prediction of thrust coefficient, power coefficient and efficiency compared to experimental analysis.

Different software may be utilized to determine the structural integrity, such as ANSYS Mechanical, and SolidWorks Static Simulation FEA. Seetharama et al. [18] performed stress analysis of composite propeller by utilizing ANSYS. The pressure was initially generated by using Fluent, and imported for structural analysis. The maximum deformation and normal stresses were then compared with the material limit. Das et al. [19] study the effect of structural deformation on performance of marine propeller blade. This is because highly deformed propeller blade may influence the hydrodynamic performance. Kishore et. al [20] conduct FEM analysis utilizing ANSYS-Workbench to determine the best material for sub-marine propeller blade. The method used in this study is discussed and the result was compared in terms of Von-Mises Stress, Von-Mises strain and total deformation for different material. In addition Yeo et al. [21] discussed blade stress distribution for marine propeller. The analyses were done by using SolidWorks Static Simulation FEA. Pressure distribution of the blade was initially obtained through CFD analysis. The resulting pressure, force and moment were then transmitted to FEA tools. The analyses were done for a range of advance ratio.

2. METHODOLOGY

APC Slow Flyer 10'x7' off-the-shelf propeller is set as standard baseline design, due to availability of experimental data [13], [14], [22]. This study focuses on two main analysis, including aerodynamic analysis and static structural analysis. The aerodynamic analysis intended to determine propeller performance in terms of thrust coefficient, power coefficient and efficiency. Initially baseline design is analyzed numerically by using computational fluid dynamic software, ANSYS Fluent. The results obtained from numerical analysis are compared with experimental data to validate numerical setup to predict propeller performance. Based on the validated method, newly developed slotted design will be analyzed and the results compared with baseline configuration. The analysis is varied based on slotted oval angle ranging from 180 degree to 90 degree.

Fig. 1 – APC Slow Flyer 10'x7' baseline design

2.1 APC Slow Flyer

APC Slow Flyer is a small-scale propeller commonly used for UAV. The blade is 10-inch in diameter with 7-inch pitch.

Based on the manufacturer data, this propeller is made up from two different airfoils namely Eppler E63 and Clark-Y for hub and tip, respectively. Fig. 1 shows the propeller three-dimensional model, created in CATIA V5.

2.2 Computational Fluid Dynamics (CFD)

2.2.1 Computational Domain

The flow domain used for this study is shown in Fig. 2. The flow domain is divided into two regions, namely stationary and rotating. The stationary region is box shape, with the distance of 4D upstream and 4D downstream as shown in Fig. 2(a). The inlet, outlet and wall section of the stationary part are set far enough to prevent recirculation of the flow which will influence the overall results of the analysis.

In addition, Fig. 2(b) shows the rotating region, which is a smaller cylinder enclosing the propeller blade entirely. The rotating region is set with 0.4 thickness and 1.1D of enclosure. The rotating region is set with Multiple Reference Frame (MRF) allowing rotation of the domain at a specific rotational speed.

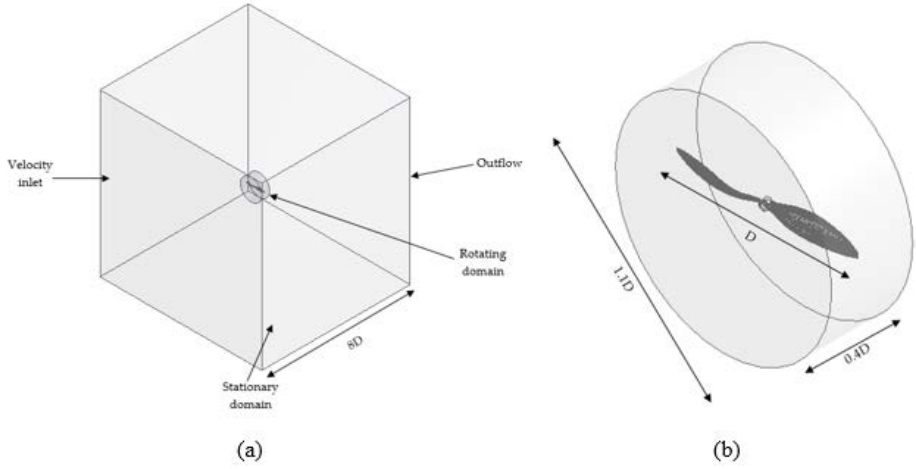

Fig. 2 – Flow domain and boundary conditions. (a) Stationary region flow domain. (b) Rotating region flow domain

2.2.2 Mesh Generation

The grid generated in this study is fully unstructured tetrahedral meshing for both stationary and rotating region. The selection of this mesh is because it requires lesser computational time and with good convergence rate as it manage to capture the flow behavior to ensure reliable results. The meshing is set to be more refined along the propeller blade section, and gradually increase outwards to the stationary region allowing more precise analysis around the boundary layer.

2.2.3 Boundary Conditions

The analyses were conducted for a range of advance ratio, varying in freestream velocity at a fixed rotational speed of 3008 RPM. Standard k-ω model is selected as the turbulence model used throughout the analysis. This is because the model is more suitable for low Reynolds number applications compared to Standard k-ε or SST k-ω.

On the inlet flow, the inlet velocity is set as tabulated in Table 1. Turbulence intensity is set to be 0.1% based on the experimental analysis tested by [13], [14], [23]. Outflow boundary conditions were specified for the outlet section downstream of the flow domain. Rotating region is set to be rotated by implying Multiple Reference Frame (MRF) model. MRF is suitable for propeller analysis as it adapts the interaction between stationary region with freestream velocity, and rotating region with specific rotating speed.

Table 1. – Simulation flow conditions

Advance coefficient, J	Freestream velocity (m/s)
0.192	2.4384
0.236	2.9972
0.282	3.5814
0.334	4.2418
0.383	4.8641
0.432	5.4864
0.486	6.1722
0.527	6.6929
0.573	7.2771
0.628	7.9756
0.659	8.3693
0.717	9.1059
0.773	9.8171
0.799	10.1473

Table 2. – Propeller blade material properties

Property	Value
Density	1690 kg/m^3
Young's Modulus	19500 MPa
Poisson's Ratio	0.44
Stress at break	250 MPa
Strain at break	1.58%

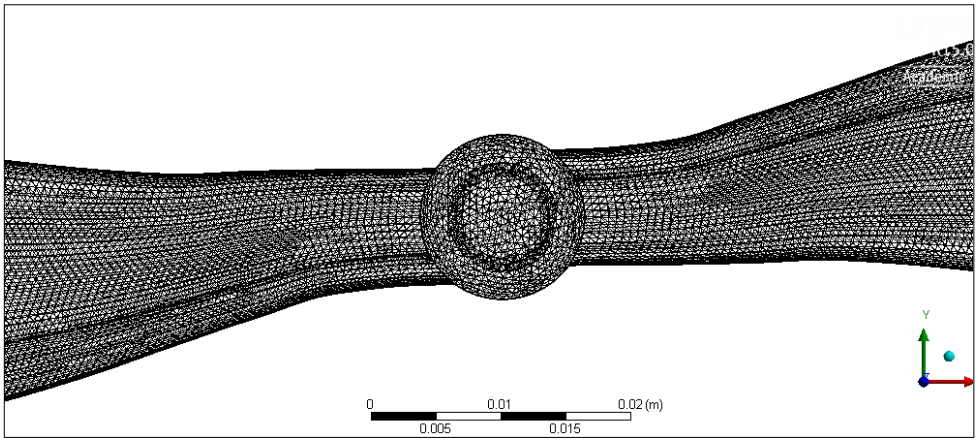

Fig. 3 – Meshing of propeller blade for static structural analysis

SIMPLE (Semi Implicit Method for Pressure Linked Equations) algorithm was specified for pressure-coupling.

Second order upwind was applied for momentum interpolating scheme, and first upwind scheme for turbulence kinetic energy and specific dissipation rate interpolation scheme.

First order upwind schemes were selected as they may provide adequate analysis with low error.

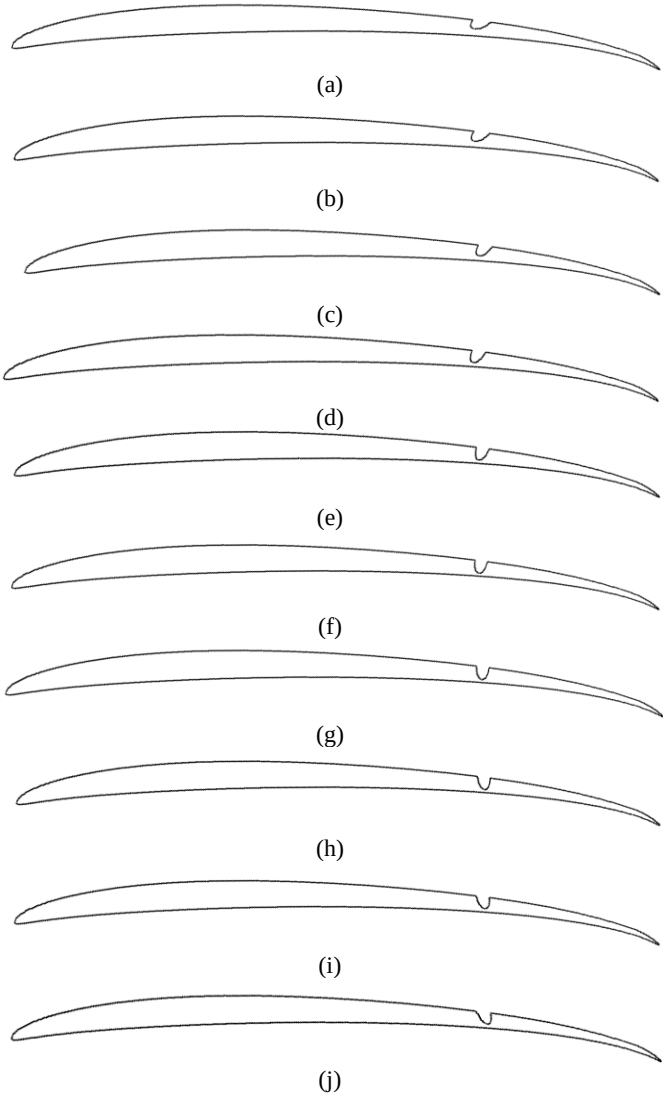

Fig. 4 – Slotted propeller blade with various blade angle. (a) Initial blade configuration, 180 degree. (b)-(j) Increment in slot angle by 10 degree respectively

2.3 Static Structural Analysis

Static structural analysis is very important, as it provide an insight on the propeller strength to withstand the forces acted along the blade. The forces that acts on the blade are specifically from thrust, torque due to aerodynamic effect and centrifugal force induced by propeller rotational motion. For this study, ANSYS Mechanical Static Structural workbench was utilized to determine maximum stress, maximum strain and total deformation of the propeller blade resulting from the force.

2.3.1 Engineering data

For the analysis, the material used for APC Slow Flyer, 60% long strand fiber glass reinforced nylon 6 Natural is set as reference material. The material properties are listed in Table 2, as retrieved from manufacturer data list [24].

2.3.2 Meshing

In this study, meshing of the propeller blade for structural analysis is generated with unstructured tetrahedral mesh. The meshes generated for the blade are shown in Fig. 3. The numbers of elements created are 213,242, with 376178 nodes. Face sizing and curvature advance size function were set for the meshing to ensure better mesh generation.

2.3.3 Boundary conditions

Pressure distribution obtained from ANSYS Fluent analysis was adopted to perform structural analysis. This allows more precise transition of pressure, force and moment based on operating freestream velocity for static structural analysis. The analyses were conducted to provide range of safe operational speed to prevent failure during operation. Von-Mises stress, Von-Mises strain obtained from the analysis were then compared with material stress and strain at break limit, as listed in Table 2.

2.4 Slotted Blade

Fig. 4 presents the design used of slotted propeller blade. Oval shape slots were used for the design and were placed at 75% from the leading edge, with respect to chord length. The chord length, diameter and pitch of the blade remain similar with APC Slow Flyer 10' x 7' allowing fair comparison between slotted and baseline design configuration. To determine the influence of slot angle, the slotted oval size is fixed with variance only in the angle with 10 degree increment from the initial configurations that is set to be 180 degree.

3. RESULTS AND DISCUSSIONS

3.1 Validation of Numerical Analysis

The thrust and power obtained from numerical analysis were validated using experimental data obtained from [13], [14], [23]. The data were calculated based on Equations (1) - (6) as listed below. Equations (1) to (4) describe thrust coefficient, power coefficient, efficiency and advance ratio, respectively. Meanwhile Equation (5) and Equation (6) show percentage change between numerical and experimental method for thrust and torque, respectively.

$$K_T = \frac{T}{\rho n^2 D^4} \tag{1}$$

$$K_P = \frac{P}{\rho n^3 D^5} \tag{2}$$

$$\eta = J\frac{K_T}{K_P} \tag{3}$$

$$J = \frac{V}{nD} \tag{4}$$

$$\Delta K_T(\%) = \frac{K_{T_{CFD}} - K_{T_{EXP}}}{K_{T_{EXP}}} \times 100 \tag{5}$$

$$\Delta K_P(\%) = \frac{K_{P_{CFD}} - K_{P_{EXP}}}{K_{P_{EXP}}} \times 100 \tag{6}$$

Based on the equations, T(N) represents thrust, P(W) is power, n (rps) rotational speed of the propeller, D (m) diameter of the propeller, ρ (kgm^{-3}) is the operational fluid density.

Fig. 5 shows the comparison for baseline design computed through numerical analysis and experimental analysis. For thrust coefficient, the result shows under-prediction for lower advance ratio, and slight over-prediction for high advance ratio. Generally, the result is influenced by advance ratio, higher advance ratio shows higher difference with experimental results.

In addition, power coefficient shows similar pattern, with slight under prediction for lower advance ratio. Highest difference with 10.75% can be seen for advance ratio of 0.192. Meanwhile for efficiency the advance ratio shows over-prediction for the whole range of advance ratio. This is because efficiency is influenced by thrust and power coefficient. Highest difference can be observed for advance ratio of 0.799, with 42.5% compared to experimental data.

3.2 Effect of Slot Angle

Fig. 6, Fig. 7 and Fig. 8 show the influence of slot angle towards propeller performance. The dimension of the slot is fixed; meanwhile the angle is changed at an interval of 10 degree from the initial slot angle that is set to be 180 degree.

The analyses were carried out for nine slot angles, specifically 180, 170, 160, 150, 140, 130, 120, 110, 100 and 90 degrees, respectively.

For a slot angle of 180 degrees, the overall thrust coefficient for slotted design is slightly reduced from baseline design. The design is approaching windmill state (negative thrust) at a lower advance ratio, compared to baseline design. In addition to reduction of thrust, the design also experiences increase power coefficient, with maximum of 24.04% for advance ratio of 0.799.

For a slot angle of 170 degrees, the results are more convincing, in which increase in thrust coefficient can be observed for a wider range of advance ratio. Maximum increase in thrust can be observed at the advance ratio of 0.192, with 2.71% increment compared to baseline design.

The blade with slotted design achieved thrust values of 0.33% to 2.71% greater than baseline design for low advance ratio condition ranging from 0.468 to 0.192, respectively. For higher advance ratio, thrust coefficient generated is lower, with reduction nearly half than baseline design.

Apart from that, power coefficient increases linearly with increase of advance ratio, compared to baseline design.

For a slot angle of 160 degrees, the design also shows increase in thrust coefficient maximum increase of 1.66% for advance ratio of 0.432. Increase in thrust can be observed for range of advance ratio of 0.192 to 0.432, with 0.2% to 1.66%. The remaining generate less thrust compared to baseline design.

However, this design experiences increase in power coefficient, ranging from 13.19% to 21.76% compared to baseline design.

For a slot angle of 150 degrees, maximum thrust generated compared to baseline design increase by 1.45% which occurs at advance ratio of 0.192.

Similarly, increment of advance ratio can be observed as lower advance ratio, ranging from 0.192 to 0.432. Lower thrust coefficient is generated for higher advance ratio, ranging from 0.486 to 0.799. Similar pattern for power coefficient can be observed, with increment of 12.47% to 25.13%.

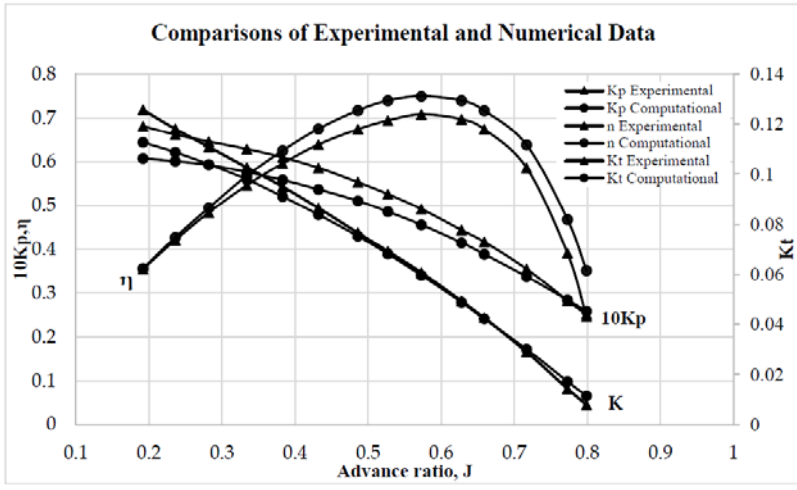

Fig. 5 – Comparisons of thrust coefficient, power coefficient, and efficiency for baseline design

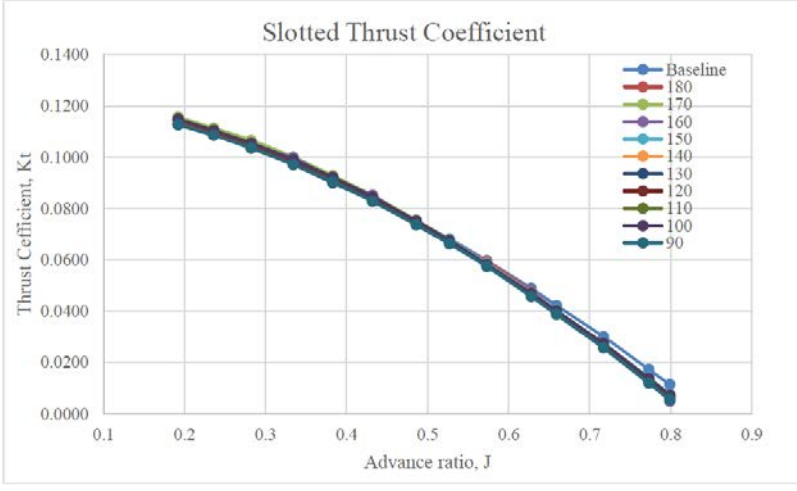

Fig. 6 – Thrust coefficient for slotted blade design for various slot angles

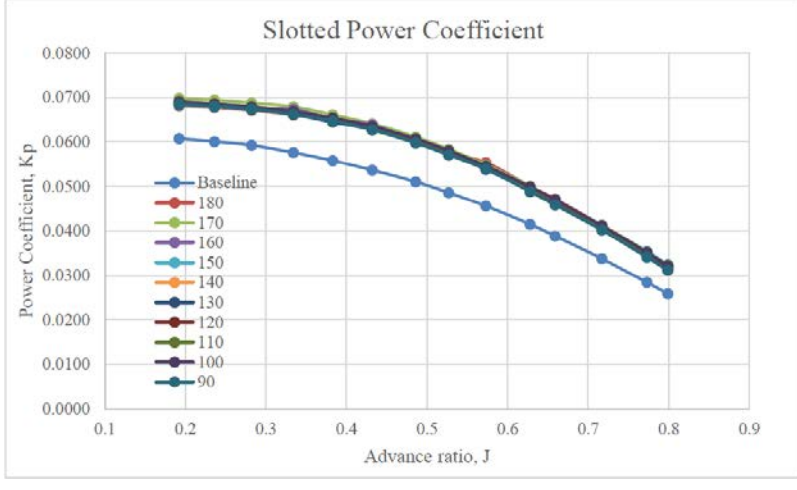

Fig. 7 – Power coefficient for slotted blade design for various angles

For a slot angle of 140 degrees, better performance can be observed compared to baseline design with increment in thrust coefficient by 0.27% to 1.41% for advance ratio of 0.432 and 0.192, respectively. For higher advance ratio, the thrust coefficient decreases with maximum reduction of advance ratio of 0.799. Furthermore, increase of power coefficient can be observed throughout the whole range of advance ratio, with minimum of 13.41% for advance ratio of 0.192, and maximum of 22.77% for 0.799.

For a slot angle of 130 degrees, the result shows performance reduction for all the range of advance ratio. Significant decrease of thrust coefficient can be observed for higher advance ratio, with reduction range of -0.15% to -42.57%. This shows that this slot angle is not suitable for performance improvement for slotted propeller. Apart from that, significant increase can also be observed for power coefficient, with increase ranging from 12.79% to 22.88% for advance ratio of 0.192 and 0.799 respectively.

For a slot angle of 120 degrees, the design also shows better performance compared to baseline design at lower advance ratio. Maximum of 1.49% can be observed for the slotted design, with minimum increment of 0.18% for advance ratio of 0.432. Higher advance ratio, ranging from 0.486 to 0.799 experiences decrease in advance ratio. Furthermore, power coefficient for slotted design is smaller than baseline design approximately around 13.93% to 36.14%.

For slot angle 110 degree, similar pattern of thrust can be observed, with increase in thrust coefficient for lower advance ratio, and further decrease in higher advance ratio compared to baseline design. The highest increase can be observed at advance ratio of 0.192, with 1.98% and minimum increase of 0.79% at advance ratio of 0.432. However, increase in thrust coefficient is also accompanied by increase in power coefficient.

For a slot angle of 100 degrees, thrust coefficient overperforms compared to thrust generated by baseline design. Highest thrust can be observed at lower advance ratio with maximum and minimum increase by 0.67% and 1.08%, respectively. At higher advance ratio, thrust coefficient reduced, compared to baseline design. Apart from that, power coefficient, maximum power coefficient change is by 23.78% at advance ratio of 0.799 and 13.45% for advance ratio of 0.192.

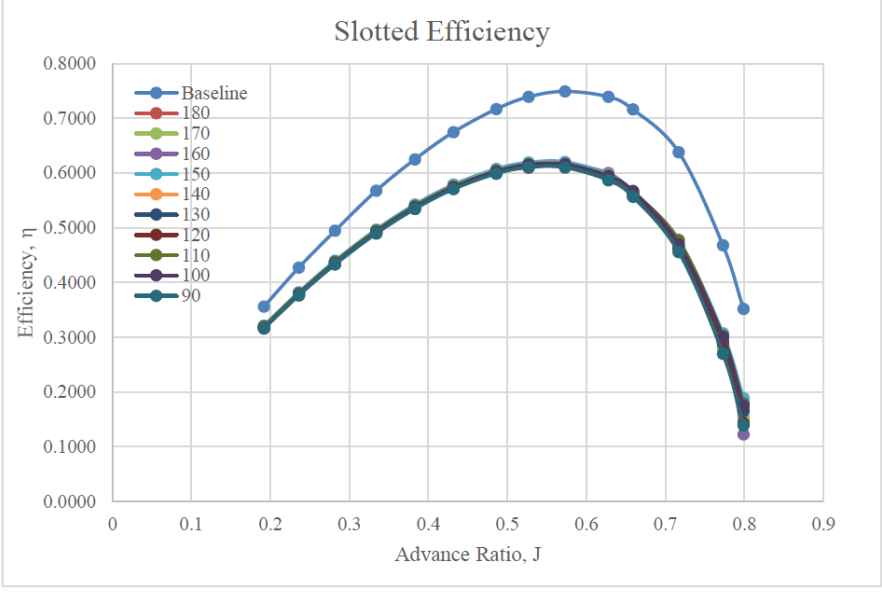

Fig. 8 – Efficiency for slotted blade design for various angles

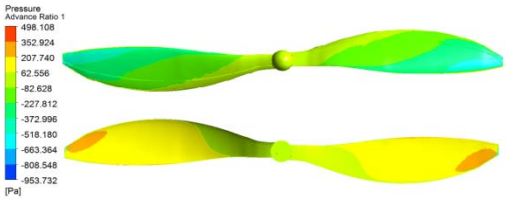

(a)

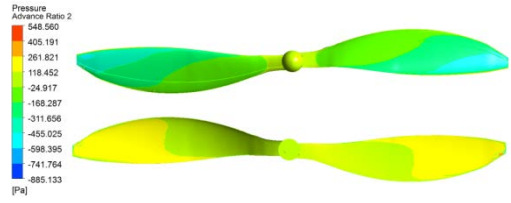

(b)

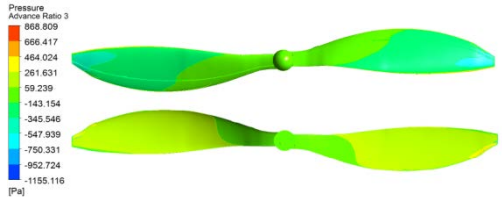

(c)

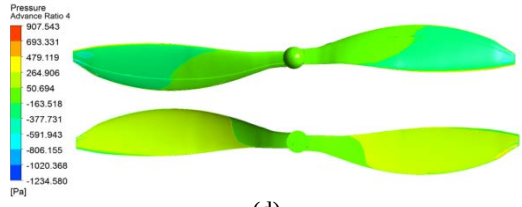

(d)

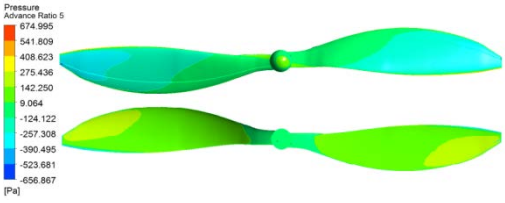

(e)

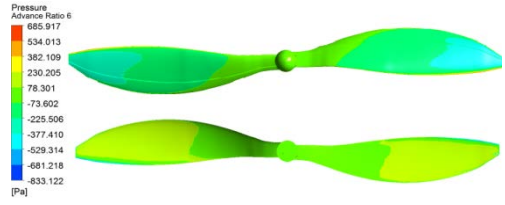

(f)

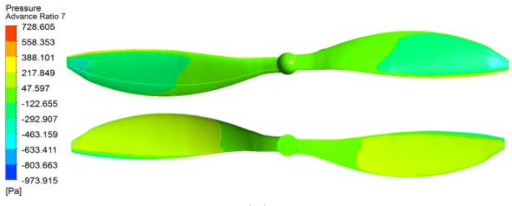

(g)

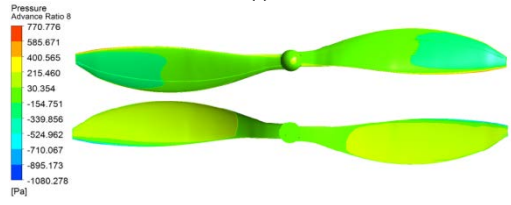

(h)

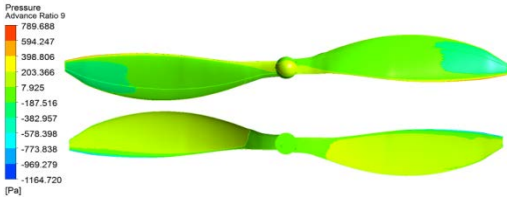

(i)

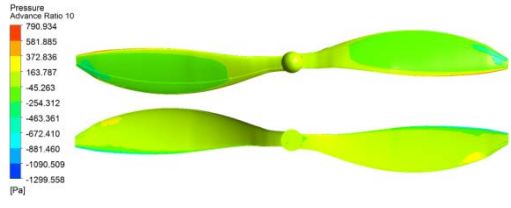

(j)

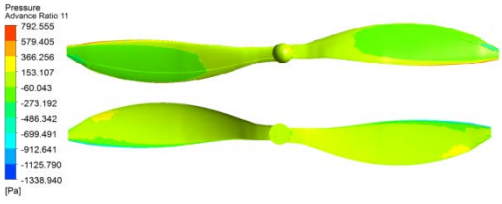

(k)

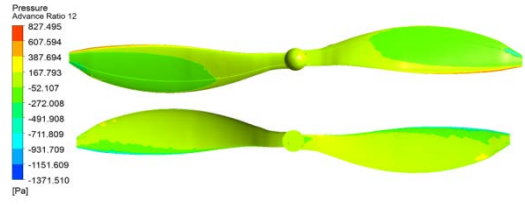

(l)

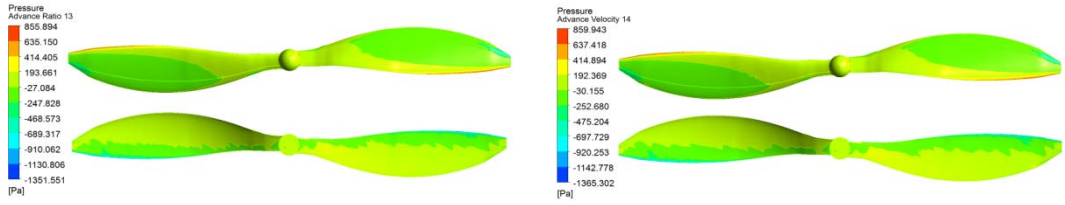

(m) (n)

Fig. 9 – (a)-(n) Propeller blade pressure distribution at various freestream velocity at 170 degrees. (Top) Pressure at the front side. (Bottom) Pressure at the back side

For a slot angle of 90 degrees, the design shows decrease in thrust coefficient over the entire range of advance ratio. At advance ratio of 0.799 reduction of more than half compared to baseline design can be observed. In addition, increase in power coefficient occurs for the design over the advance ratio.

Based on the result discussed above, for most of the slotted oval propeller blade angle, the thrust coefficient managed to provide performance improvements for lower advance ratio, ranging from 0.192 to 0.432. Meanwhile, for higher advance ratio, it is prone to experience lower blade performance. In addition, inducing slotted into the design causes higher power coefficient, thus, reducing the performance of the blade as illustrated in Fig. 8.

Reduction in propeller efficiency occurs because it is directly influenced by thrust and power performance, as described in Equation 4. Although thrust increases for lower advance ratio, but it is accompanied by increase in drag, thus bound to decrease in the efficiency.

Therefore, based on the result discussed, induction of oval slotted design with various angle does not always lead to performance improvements. For most of the cases, although the thrust increase, reduction of efficiency opposed the main objective of the design. The reduction is predicted to occur mainly because the flow might not be able to be pushed back into the flow to alter the boundary layers and flow separations.

3.3 Pressure Distribution

From CFD analysis, pressure distribution along the blade is generated. The pressure distribution data collected will be further used in ANSYS Mechanical for Static Structural analysis. Slotted blade angle of 170 degrees was selected to be further discussed in terms of pressure and static structure as it provides the best performance among the other slot angles. Maximum and minimum pressure is tabulated in Table 3.

Fig. 9 shows the pressure contour for slot angle of 170 degrees at various freestream velocity, as listed in Table 1. Generally, the pressure loading at the back side of the propeller and the front side of the propeller pushes the air to thrust it forward. The pressure generated is basically due to the airfoil profile and blade angle implemented on each section of the propeller blade. In addition, leading edge of the blade experience higher pressure compared to the trailing edge, because of stagnation point.

Apart from that, the velocity highly influences the pressure distribution. Higher velocity will experience lower pressure difference thus, lower thrust generation throughout the blade. At velocity of 2.438m/s, positive pressure generated is 498 Pa, while negative pressure reached is 953 Pa. As the velocity is higher, the negative pressure continued to increase on the front section of the propeller blade. In addition, smaller region of negative pressure can be observed at the back of trailing edge due to the airflow.

Table 3. – Maximum and minimum pressure for slotted design

Freestream velocity (m/s)	Pressure (Pa)	
	Maximum	Minimum
2.4384	498.108	-953.732
2.9972	548.56	-885.133
3.5814	868.809	-1155.116
4.2418	907.543	-1234.58
4.8641	674.995	-656.867
5.4864	685.917	-833.122
6.1722	728.605	-973.915
6.6929	770.776	-1080.278
7.2771	786.688	-1164.72
7.9756	790.934	-1299.558
8.3693	792.555	-1338.94
9.1059	827.495	-1371.51
9.8171	855.894	-1351.551
10.1473	859.943	-1365.302

3.4 Stress Distribution and Deformation of Propeller Blade

Stress analysis was conducted by using ANSYS Static Structural to determine the structural behavior of the blade in terms of Von-Mises Stress, maximum Von-Mises Strain and total deformation.

The obtained stress distribution is illustrated in Fig. 10, and the details were tabulated in Table 4. Generally, all blades have similar stress distribution along the blade with each freestream velocity.

Thus, only stress distribution for velocity of 2.438m/s was presented. As shown in Fig. 10, stress is concentrated near to the hub, and reduces as it moves along the tip. In addition, as the velocity increases, the stress acted on the blade decrease.

This is because the force acted on the propeller blade will directly influence the generated stress.

To estimate structural integrity of the blade during operation, the stress generated was compared with the stress at the brake point based on material selected, discussed in Section 2.3.1. Based on the results, for this design and material selected, it is more suitable to operate at higher velocity.

This is because at higher velocity, the stress generated is below the stress at breaking point for the material. Similar behavior occurs for maximum strain, in which the blade is more likely to face material failure at lower operational velocity.

In addition, Fig. 11 describes the deformation profile for propeller blade operating at velocity of 2.438m/s.

The blade experiences deflection due to aerodynamic load along the blade. Based on Fig. 10, maximum deflection will occur at the tip of the blade, as it is the farthest free end section. The maximum deformation for the blade decreases with decrease in operational velocity.

Table 4.–Summary for static structural analysis

Freestream velocity (m/s)	Maximum Von-Mises Stress (MPa)	Maximum Von-Mises Stress (%)	Total Deformation (m)
2.4384	391.31	2.01	0.056
2.9972	380.02	1.95	0.054
3.5814	389.83	1.94	0.055
4.2418	376.61	1.93	0.052
4.8641	325.64	1.67	0.046
5.4864	304.09	1.58	0.042
6.1722	275.37	1.42	0.038
6.6929	247.6	1.27	0.035
7.2771	213.58	1.03	0.031
7.9756	190.47	0.98	0.026
8.3693	168.84	0.87	0.023
9.1059	134.22	0.69	0.018
9.8171	92.78	0.48	0.012
10.1473	74.16	0.38	0.0094

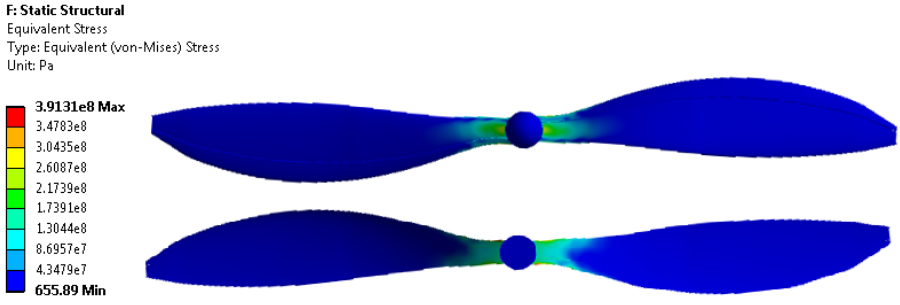

Fig. 10 – Propeller blade stress distribution. (Top) Front section (Bottom) Back section at freestream velocity of 2.4384 m/s

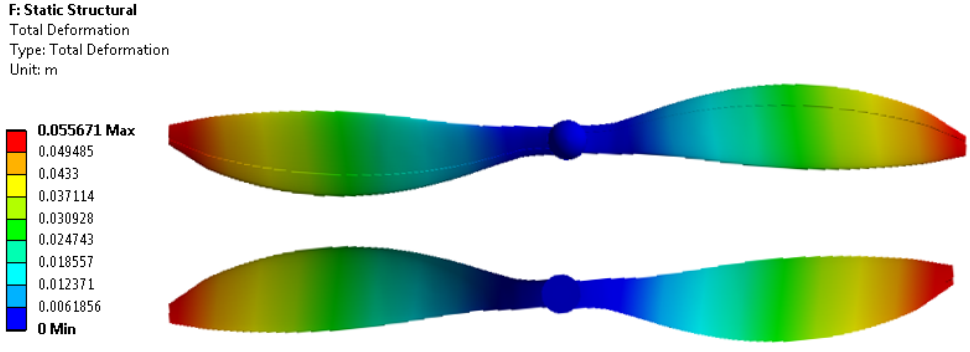

Fig. 11 – Deflection of propeller blade at freestream velocity of 2.4384 m/s

4. CONCLUSIONS

The use of slotted airfoil for performance improvement has been discussed in details in terms of aerodynamic and structural analysis. Based on the results discussed above, it can be clearly seen that operational free-stream velocity plays an important role on the overall performance of the propeller blade. Thrust coefficient increases for low advance ratio, but is also accompanied by increase in power coefficient. This leads to decrement of overall efficiency of the blade. Thus, it can be concluded that inducing slotted design does not always lead to improvement in propeller blade performance. Moreover, the stress and total deformation analysis describes that the material selected, 60% long strand fiber glass reinforced nylon 6 Natural is not rigid enough to overcome higher stress at high operational speed. This suggests that material selection for the propeller gives a significant impact, thus better material is required for this design. More rigid material is highly suggested for the propeller blade, as it may withstand load acted on it. Overall, the stress and total deformation decrease with increase in operational speed is mainly due decrease in aerodynamic load acted along the blade. Different slot size and location can be further analyzed to determine the optimized design that can improve the overall performance without losing the structural integrity.

REFERENCES

[1] R. L. Finn and D. Wright, Unmanned aircraft systems: Surveillance, ethics and privacy in civil applications, *Comput. Law Secur. Rev.*, **28** (2), pp. 184–194,https://doi.org/10.1016/j.clsr.2012.01.005, 2012.

[2] G. Pajares, Overview and Current Status of Remote Sensing Applications Based on Unmanned Aerial Vehicles (UAVs), *Photogramm. Eng. Remote Sens.*, **81** (April), 281–330,https://doi.org/10.14358/PERS.81.4.281, 2015.

[3] S. G. Kontogiannis and J. A. Ekaterinaris, Design, performance evaluation and optimization of a UAV, *Aerosp. Sci. Technol.*, **29**(1), pp. 339–350,https://doi.org/10.1016/j.ast.2013.04.005, 2013.

[4] P. Panagiotou, I. Tsavlidis, and K. Yakinthos, Conceptual design of a hybrid solar MALE UAV, *Aerosp. Sci. Technol.*, **53**, 207–219,https://doi.org/10.1016/j.ast.2016.03.023, 2016.

[5] H. C. Watts,*The design of screw propellers: with special reference to their adaptation for aircraft*, First. Forgotten Books, 1920.

[6] Q. R. Wald, The aerodynamics of propellers, *Prog. Aerosp. Sci.*, **42**(2), 85–128,https://doi.org/10.1016/j.paerosci.2006.04.001, 2006.

[7] X. Liu, H. Jawahar, M. Azarpeyvand, and R. Theunissen, Aerodynamic and Aeroacoustic Performance of Serrated Airfoils, *21st AIAA/CEAS Aeroacoustics Conf.*, June, 1–16, 2015.

[8] T. P. Chong and P. F. Joseph, An experimental study of airfoil instability tonal noise with trailing edge serrations, *J. Sound Vib.*, **332**(24), 6335–6358,https://doi.org/10.1016/j.jsv.2013.06.033, 2013.

[9] T. P. Chong and A. Vathylakis, On the aeroacoustic and flow structures developed on a flat plate with a serrated sawtooth trailing edge, *J. Sound Vib.*, **354**, 65–90. https://doi.org/10.1016/j.jsv.2015.05.019, 2015.

[10] M. Ibrahim, A. Alsultan, S. Shen, and R. S. Amano, Advances in Horizontal Axis Wind Turbine Blade Designs: Introduction of Slots and Tubercle, *J. Energy Resour. Technol.*, **137**(5), 51205. https://doi.org/10.1115/1.4030399, 2015.

[11] S. Y. Lin, Y. Y. Lin, C. J. Bai, and W. C. Wang, Performance analysis of vertical-axis-wind-turbine blade with modified trailing edge through computational fluid dynamics, *Renew. Energy*, **99**, 654–662. https://doi.org/10.1016/j.renene.2016.07.050, 2016.

[12] R. Belamadi, A. Djemili, A. Ilinca, and R. Mdouki, Aerodynamic performance analysis of slotted airfoils for application to wind turbine blades, *J. Wind Eng. Ind. Aerodyn.*, **151**, 79–99. https://doi.org/10.1016/j.jweia.2016.01.011, 2016.

[13] J. B. Brandt and M. S. Selig, Propeller Performance Data at Low Reynolds Numbers, *49th AIAA Aerosp. Sci. Meet.*, January, pp. 1–18, 2011.

[14] R. W. Deters, G. K. Ananda Krishnan, and M. S. Selig, Reynolds Number Effects on the Performance of Small-Scale Propellers, in *32nd AIAA Applied Aerodynamics Conference*, June, 2014.

[15] S. Subhas, CFD Analysis of a Propeller Flow and Cavitation, *Int. J. Comput. Appl.*, **55**(16), 26–33. 10.5120/8841-3125(2012).

[16] X. Wang and K. Walters, Computational analysis of marine-propeller performance using transition-sensitive turbulence modeling, *J. Fluids Eng.*, **134**(7), 71107-1-71107–10. https://doi.org/10.1115/1.4005729, 2012.
[17] Ã. Ernesto Benini, Significance of blade element theory in performance prediction of marine propellers, *Ocean Eng.*, **31**, 957–974,https://doi.org/10.1016/j.oceaneng.2003.12.001, 2004.
[18] Y. Rao Seetharama, K. Rao Mallikarjuna, and B. Sridhar Reddy, Stress analysis of composite propeller by using finite element Analysis, *Int. J. Eng. Sci. Technol.*, **4**(8), 3866–3875, 2012.
[19] H. N. Das, P. V. Rao, C. Suryanarayana, and S. Kapuria, Effect of Structural Deformation on Performance of Marine Propeller, *J. Marit. Res.*, **X**(3), 47–50, 2013.
[20] S. Jaya Kishore, B. S. Rao, and P. K. Babu, FEM Analysis on Submarine Propeller Blade for Improved Efficiency by using Solid Works and ANSYS-Workbench, *Int. J. Emerg. Eng. Res. Technol.*, **3**(11), 144–151, 2015.
[21] K. Beng Yeo, W. Heng Choon, and W. Y. Hau, Prediction of Propeller Blade Stress Distribution Through FEA, *J. Appl. Sci.*, **14**(22), 3046–3054,http://dx.doi.org/10.3923/jas.2014.3046.3054, 2014.
[22] * * * UIUC, *UIUC Airfoil Data Site*, [Online], Available: http://m-selig.ae.illinois.edu/ads.html, Accessed on 02-Nov-2016.
[23] J. B. Brandt, R. W. Deters, G. K. Ananda, and M. S. Selig, *UIUC Propeller Data Site*, [Online], Available: http://m-selig.ae.illinois.edu/props/propDB.html, Accessed on 01-Nov-2016.
[24] * * * C. Corporation, *Celanese Technical Data*, [Online], Available: https://www.celanese.com/, Accessed on 23-Feb-2016.